A Particle-in-Cell Simulation of a Cyclic Beam Buncher

ANTHONY L. PERATT, SENIOR MEMBER, IEEE, CHARLES M. SNELL, AND FRANKLIN S. FELBER, MEMBER, IEEE

Abstract—**A relatively weak TE wave in a cylindrical cavity can efficiently bunch an intense electron beam when the phase velocity of the wave is matched to the beam cyclotron frequency. Fully electromagnetic, relativistic, 2-½-dimensional simulations illustrate the applicability of this bunching mechanism to high-power generators.**

I. Introduction

IN HIGH-POWER electron-beam generators and accelerators, the pulse length operating range is largely constrained by the acceleration mechanism. Many such devices have pulse lengths in the range 30–300 ns with little flexibility. A cyclic beam buncher may provide a simple and effective means for extending the applicability of large generators and accelerators to short pulse operating ranges and higher peak powers [1]. In addition, a bunched relativistic electron beam (REB) is a copious producer of microwaves, and the wave–beam interaction mechanism may provide insights on why large amounts of power have been measured in circulating modes in magnetically insulated transmission-line oscillators (MILO's) [2], [3].

Conventional beam-buncher concepts typically involve high-power momentum modulation followed by a long drift region in which bunching occurs. In a cyclic beam buncher, an electromagnetic wave circulates synchronously with the beam and causes the electrons at different wave phases to travel different path lengths so that the electrons bunch at the nodes of the wave. The cyclic beam buncher has certain advantages in size and power requirements. Both momentum modulation and bunching are accomplished within the same cavity to achieve compactness. Power requirements are low because the physical bunching mechanism is an exchange of kinetic energy from some electrons to others in the beam, through an intermediary electromagnetic field.

The geometry under consideration is shown in Fig. 1. A wave circulates in an axisymmetric cylindrical cavity. The electron beam is confined radially and axially by an external magnetostatic betatron field B_{z0}, and is bunched by the azimuthal electric field of the wave E_θ, which must be greater than approximately the voltage spread in the beam divided by the wavelength. The wave phase velocity is synchronized with the average azimuthal beam velocity v_θ. Typically, less than one revolution suffices to bunch the beam.

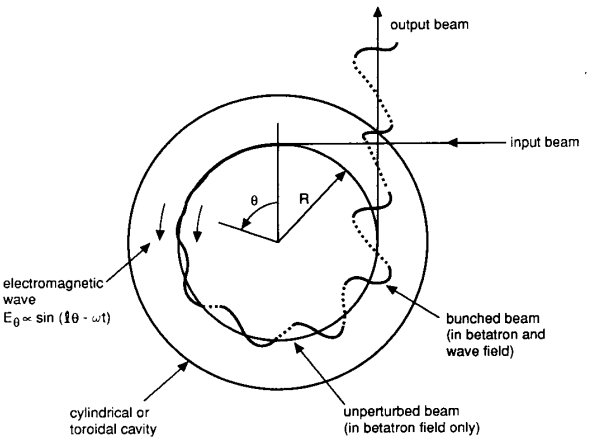

Fig. 1. Schematic of cyclic beam buncher.

Once the beam is bunched, it may be extracted for direct applications or used to produce microwave radiation. If it is to be extracted, the emittance may be minimized by extracting the beam only at particular values of the phase. If the beam is to be used to generate microwaves, the same cavity in which the beam is bunched may be used to amplify the wave that produced the bunching.

II. Transverse Electric Cavity Modes

In terms of the transverse-electric propagating wave function [4]

$$\psi_{npq}^{\mathrm{TE}} = E_0 J_n\left(\frac{x'_{np} r}{a}\right)\begin{Bmatrix}\sin n\theta \\ \cos n\theta\end{Bmatrix} \sin(qnz/d)\exp(-i\omega t) \tag{1}$$

the electromagnetic cavity fields are

$$E_r = \frac{1}{r}\frac{\partial \psi}{\partial \theta} \tag{2}$$

$$E_\theta = \frac{\partial \psi}{\partial r} \tag{3}$$

$$E_z = 0 \tag{4}$$

Manuscript received September 28, 1989; revised February 6, 1990.

A. L. Peratt and C. M. Snell are with the Los Alamos National Laboratory, X-10, MS-B259, Los Alamos, NM 87545.

F. S. Felber is with JAYCOR, P.O. Box 85154, San Diego, CA 92138.

IEEE Log Number 9035695.

$$H_r = \frac{1}{\hat{z}} \frac{\partial^2 \psi}{\partial r \, \partial z} \tag{5}$$

$$H_\theta = \frac{1}{\hat{z} r} \frac{\partial^2 \psi}{\partial \theta \, \partial z} \tag{6}$$

$$H_z = \frac{1}{2} \left(\frac{\partial^2 \psi}{\partial z^2} + k^2 \right) \tag{7}$$

where $n = 0, 1, 2, \cdots, p = 1, 2, 3, \cdots$, and $q = 1, 2, 3, \cdots$, refer to azimuthal, radial, and axial field variations, respectively. The bracketed term in (1) denotes that any linear combination of sin $n\theta$ and cos $n\theta$ may be chosen for a solution to a particular problem. The quantities x'_{np} are the ordered zeros of the Bessel function derivative $J'_n(x'_{np})$. The parameter $\hat{z}(\omega) = -i\omega\mu$, for a medium of inductivity μ is the impedivity of the medium. The dispersion equation for a cavity of height d and radius a is

$$\left(\frac{x'_{np}}{a} \right)^2 + \left(\frac{q\pi}{d} \right)^2 = k^2.$$

The cavity fields are introduced into the simulation code field solver by specifying the initial azimuthal and radial fields. A suitable choice of field solutions is

$$E_r = -\frac{n}{r} E_o J_n(x'_{np} \, r/a) \cos(n\theta - \omega t) \sin(qnz/d) \tag{8}$$

$$E_\theta = -\frac{x'_{np}}{a} E_o J'_n(x'_{np} r/a) \sin(n\theta - \omega t) \sin(qnz/d). \tag{9}$$

Additionally, the time derivatives of the fields are

$$\frac{dE_r}{dt} = -\omega \frac{n}{r} E_o J_n(x'_{np} r/a) \sin(n\theta - \omega t) \sin(qnz/d) \tag{10}$$

$$\frac{dE_\theta}{dt} = +\omega \frac{x'_{np}}{a} E_o J'_n(x'_{np} r/a) \cos(n\theta - \omega t) \sin(qnz/d) \tag{11}$$

which are used for time update of the external electric fields in the simulation field-solving routine [5], [6]. Once the electric fields are specified, the magnetic field components are calculated from the equation $\partial \boldsymbol{B}/\partial t = -\nabla \times \boldsymbol{E}$.

The field normalization, the knowledge of which is required to scale the simulation field strengths, depends on the cavity mode excited and is given by

$$E_0 = \frac{E^{\mathrm{TE}}_{\theta npq}}{\frac{x'_{np}}{a} J'_n\left(\frac{x'_{np} r}{a} \right)}. \tag{12}$$

III. Simulation Setup

The computer simulations were performed with the ISIS and MERLIN codes [5], [6]. MERLIN is a fully electromagnetic, relativistic, particle-in-cell plasma simulation code that runs in two spatial dimensions with three momentum components per particle. The code can be used in a wide variety of coordinate systems, including cartesian x-$y(z)$, cylindrical z-$r(\theta)$, and cylindrical-polar r-$\theta(z)$. In each case the omitted coordinate has been enclosed in parentheses. For the present problem, the cylindrical-polar coordinate system is relevant. In this system, there is an implicit assumption of axial uniformity ($\partial/\partial z \rightarrow 0$). MERLIN also permits the use of a wide variety of boundary conditions: conducting, open, wave-transmitting, and periodic. Internal conductors (perfect and imperfect) and dielectrics may also be used and, optionally, moved. For the simulations reported in this paper, a conducting outer boundary was employed, and the internal medium was taken to be a vacuum. Although MERLIN does treat beam space charge effects, such effects are small for the examples chosen.

A. Coordinate Specification

Electromagnetic simulations in the r-θ plane are subject to a severe Courant limit on the time step because of the very small spatial size of the cells near the origin. We therefore introduce a transformation in the radial coordinate that increases the size of cells near the axis relative to the size of cells in the vicinity of the layer. The transformation we use [7] is

$$s = \frac{a_o^2}{2} \ln\left(1 + \frac{r^2}{a_o^2} \right) \tag{13}$$

where r is the true radial coordinate, s is the transformed computational coordinate, and the smallest cells are near $r = a_0$. Another way of avoiding this problem, of course, is to omit simulating the region near the axis. We choose to include the axis in order to simulate an experiment lacking a central conductor; a high degree of beam bunching can push particles towards the interior of the cavity. Additionally, (13) allows for the simulation of both cylindrical and toroidal cavities. In the r-θ plane, the region $0 \leq \theta \leq 2\pi$, was discretized with 100×64 cells. Fig. 2 shows the spatial finite-difference grid resulting from this discretization and (13).

B. Simulation Parameters

As an example, we consider a 35-MeV ($\gamma = 69$) electron beam having a radial temperature of 70 keV and injected into a 0.28-m-radius cavity at a radial position of 0.14 m from the cavity center.

The magnetostatic field necessary to confine this beam at 0.14 m radius is about 0.85 T, so that the relativistic gyrofrequency $\Omega_c = eB_0/\gamma$ m is $2 \cdot 10^9$ s^{-1}. Beam thicknesses were varied from $\Delta r = 2$ to $\Delta r = 8$ mm, and the average particle density was $n_0 = 5 \cdot 10^{10}$ cm^{-3}. The

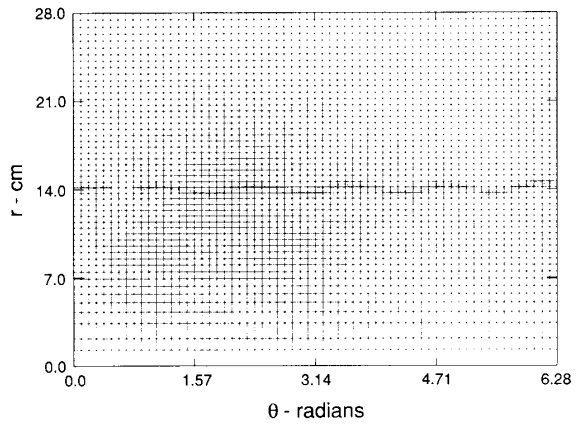

Fig. 2. Spatial grid. Finest zoning is at $r = 0.155$ m, approximate spatial average position of bunched beam at extraction time. For reference, electron beam injected at radius of 0.14 m is shown at early times.

reference value (at $\gamma = \gamma_0$ and $n = n_0$) of the relativistic plasma frequency, $\omega_p \equiv (e^2 n_0/\epsilon_0 \gamma_0 m)^{1/2}$, was $5 \cdot 10^9$ s^{-1}, so that the ratio ω_c/ω_p was 0.4.

The time step for the calculation was chosen very small, $\delta t = 10^{-12}$ s, so that high harmonics of all relevant frequencies were well resolved.

The condition that the trapping width be wide enough for most particles to be trapped [1] is

$$n\left(\frac{\Delta\gamma_{th}}{\gamma}\right)B_0 < E_0/c < \frac{1}{n}\left(\frac{1-s}{2}\right)^2 B_0 \qquad (14)$$

where $\Delta\gamma_{th}/\gamma$ is the beam thermal spread and s is the betatron field index. For the parameters listed in Table I, and for azimuthal mode $n = 5$, the inequality becomes 2 MV/m $\lesssim E_0 \lesssim$ 10 MV/m. Synchronism between the wave phase velocity and the beam velocity $v_b \approx c$ requires

$$\omega = n\Omega_c \qquad (15)$$

or, for $n = 5$, $\omega = 1.07 \times 10^{10}$ s^{-1}, or $f = 1.7$ GHz.

C. Electron Layer Confined by Magnetostatic Betatron Field

To start the simulation, we require the presence of a relativistic charged particle layer in rotational equilibrium under an imposed axial betatron magnetic field. The first task for the simulation code then is to obtain a numerical solution for that equilibrium. We use the method outlined by Gisler [7].

Although the particles in the layer may have a finite temperature, we nelgect it in obtaining the equilibrium solution. We assume that the flow is laminar and that the particles have no axial or radial motion. Each particle is thus assumed to be in equilibrium at its own radial position. The equations that must be solved are

$$\frac{1}{r}\frac{d}{dr}(rE_r) = \rho/\epsilon_0 = qn(r)/\epsilon_0 \qquad (16)$$

TABLE I
SIMULATED CYCLIC BEAM BUNCHER

Beam energy	35 MeV ($\gamma = 69$)
Radial temperature of electrons	70 keV
Beam energy spread	$\Delta\gamma/\gamma = 0.002$
Beam major radius	0.14 m
Beam width	8, 2 mm
Beam current	120, 7.5 A
Cavity radius	0.28 m
Magnetostatic field, B_{z0}	0.85 T
RF mode	TE_{511}
RF field at beam	1, 2 MV/m
RF field maximum	2, 4 MV/m
Interaction angle	$(5/6)2\pi$
$(5/6)2\pi$ cycle time	2.44 ns
Bunch separation on output	0.587 ns

$$\frac{dB_z}{dr} = -\mu_0 J_\theta = -\mu_0 qn(r)\beta c \qquad (17)$$

$$q(E_r + \beta c B_z) + \gamma m v_\theta^2/r = 0 \qquad (18)$$

where $\beta = v_\theta/c$, $\gamma = (1 - \beta^2)^{-1/2}$ is the relativistic Lorentz factor, and m and q are the particle mass and charge, respectively.

The equilibrium solver in the code works as follows: given a density profile $n(r)$, we numerically integrate (16) to obtain the radial electric field profile. An initial guess for the particle energies is found by taking the energy required for a single particle to maintain a circular orbit at the desired average radius r_0 in the imposed magnetic field B_0:

$$\gamma_0 = \left(\frac{|q|B_0}{mc}\right)r_0. \qquad (19)$$

We then correct this guess for the space-charge depression of the particle energies as a function of radius, using the electric field profile already calculated. The velocities obtained from the space-charge-depressed energies are used in (17) to calculate the diamagnetic depression of the magnetic field interior to the layer (preserving the total magnetic flux). Equation (18) is then solved for the specific particle momentum, $u = \gamma\beta$, and the solution is used to obtain a new guess for $\gamma(r)$. Iteration continues between (17) and (18) until convergence is satisfactory, usually in less than ten iterations. This system of equations is solved in a similar manner by Chernin and Lau [8].

IV. SIMULATIONS

At time zero, a circulating electromagnetic wave in a TE mode is established in the cylinder. Fig. 3 shows the contours of the RF field components at $t = 0$. The polarity of every other contour changes, and the field propagates to the right (positive θ direction) in the figure.

Fig. 4 depicts the magnitude of E_θ at spatial locations corresponding to the maximum field strength and the field strength at the location of the unperturbed beam. For a peak field amplitude of 4 MV/m in a TE_{511} mode, a beam injected at 0.14 m sees, approximately, a ± 2 MV/m modulation field.

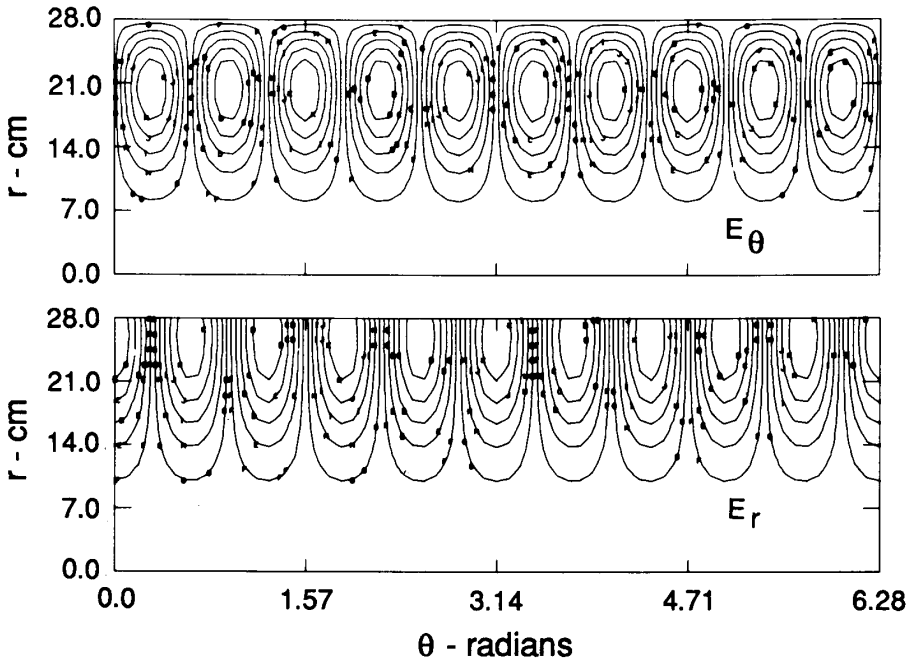

Fig. 3. Contours of E_θ and E_r. Every other contour reverses polarity with maximum amplitude of ± 4 MV/m. Fields propagate to the right.

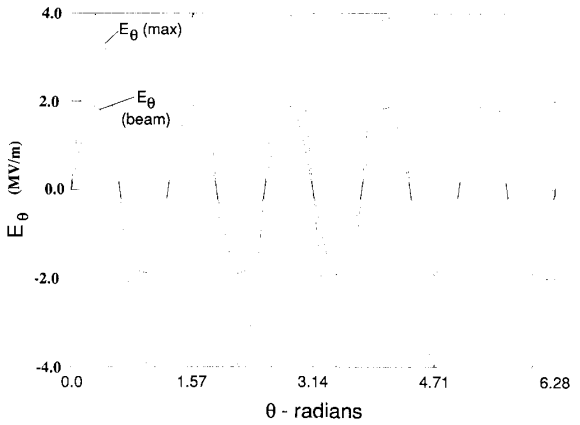

Fig. 4. Magnitude of E_θ versus θ at peak field amplitude (through peaks of contours shown in Fig. 3), and field amplitude at 0.14 m (radius of injected beam). These waveforms travel to the right.

Fig. 5 shows the time evolution of the beam electrons through an angle $\theta = (5/6)2\pi$. The beam is injected at the first time step of the simulation. In an experimental situation, an REB would be injected through a port in a field-free region of the cylindrical cavity. After 5/6 of a revolution, the bunched beam would be extracted from a port in the same field-free region. The "cylindrical" cavity might even be only a 300° resonant cavity to facilitate injection and extraction. Moreover, the "cylindrical" cavity might have a slight helical pitch to avoid interference of the extracted beam with the injected beam. In the $r - \theta$ code, this "injection" is mocked by placing a REB at the injection radius and assuring that it is in equilibrium, as described in Section III-C. We have found it convenient, for diagnostics reasons, to inject a beam that is 2.44 ns in length; i.e., corresponding to an angle $\theta = 5/6(2\pi)$. This situation is shown in Fig. 5(a). In an actual experiment, the injected beam might be 30–300 ns in length.

Because of the RF circulating wave, the propagating beam traveling in the same counter-clockwise (positive θ) direction is modulated by the wavefield. At time $t \approx 1$ ns (Fig. 5(d)), the pentagonal profile resulting from the TE_{511} RF mode is apparent.

Beyond 1 ns, the beam begins to bunch, reaching a maximum index of modulation of 6.3 (ratio of densities in the bunched and tenuous beam regions) at 2.44 ns. In agreement with the simple analysis [1], the simulations show that if the beam were not extracted at 2.44 ns ($\theta = (5/6)2\pi$), the lateral bunches would tend to fold and spread out the bunched electrons in the azimuthal direction, thereby debunching the beam.

The bunching period is

$$\tau_b = 2\pi/\omega$$

and for an RF frequency $f = 1.7$ GHz, the bunch separation at the "output" ($\theta = (5/6)2\pi$) is 0.587 ns.

Fig. 6 shows the evolution of the same injected beam but with the peak RF wave amplitude reduced from 4 to 2 MV/m. For this case the field amplitude at the beam is approximately 1 MV/m and the beam is only marginally

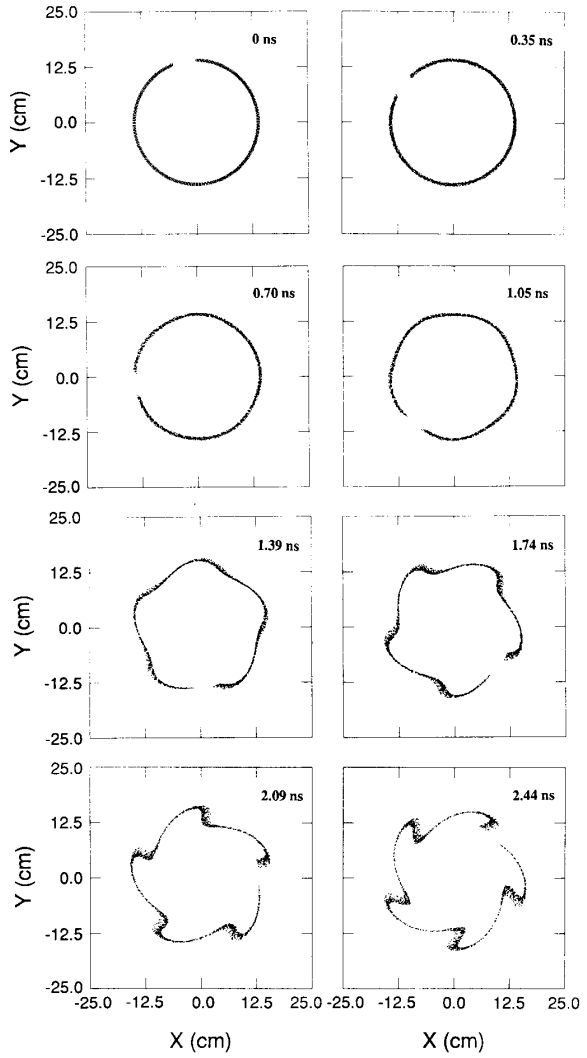

Fig. 5. Relativistic electron beam ($\gamma = 69$) at times $t = 0$, 0.35, 0.70, 1.05, 1.39, 1.74, 2.09, and 2.44 ns. Maximum RF wave amplitude at beam ~ 2 MV/m; RF frequency is 1.7 GHz.

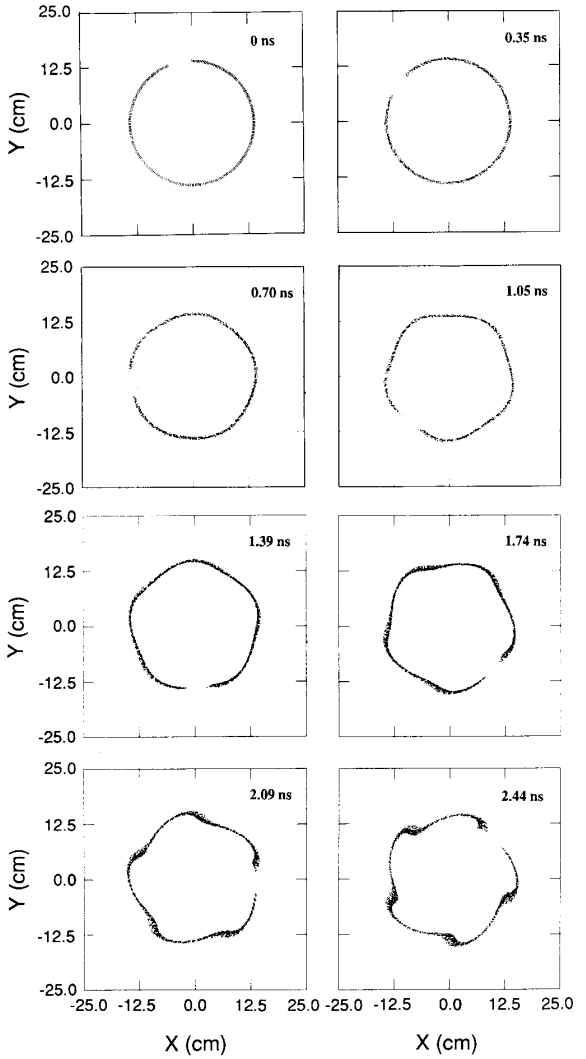

Fig. 6. Relativistic electron beam ($\gamma = 69$) at times $t = 0$, 0.35, 0.70, 1.05, 1.39, 1.74, 2.09, and 2.44 ns. Maximum RF wave amplitude at beam ~ 1 MV/m; RF frequency is 1.7 GHz.

bunched. For a static wave, a wave amplitude of 10 MV/m is required to achieve density modulation. These results are in good agreement with the resonant-like conditions specified by (14) and (15).

A cyclic beam buncher was also simulated in the TE_{211} mode with corresponding agreement found with the theoretical predictions of [1].

V. Conclusion

Cyclic beam bunching has been demonstrated in a numerical simulation of a 35-MeV ($\gamma = 69$), 4.2-GW relativistic electron beam injected into a cylindrical cavity in which a TE RF mode is circulating. For a 4-MV/m peak field amplitude in the TE_{511} mode and an RF frequency of 1.7 GHz, a modulation index of 6.3 was achieved, with beam bunches appearing every 0.6 ns at the plane of maximum interaction angle, $\theta = (5/6)2\pi$ rad.

The simulation results were found to be in close agreement with the linear single-particle theoretical results of [1]. Also in agreement with [1], the simulations showed that low-emittance beam bunching is possible as long as the RF-field energy dominates the self-field energy of the bunched beam.

References

[1] F. S. Felber, T. Tajima, and J. L. Vomvoridis, "Cyclic beam bunchers and wave generators," in *Proc. Int. Conf. on High-Power Particle Beams* (San Francisco, CA), Sept. 12–14, 1983, pp. 568–571.

[2] A. L. Peratt and M. G. Sheppard, "Power flow and microwave generation in magnetically insulated transmission line oscillators," in *Conf.*

Record 88CH2559-3, IEEE Int. Conf. on Plasma Science (Seattle, WA), June 6–8, 1988, p. 99.
[3] A. L. Peratt and M. G. Sheppard, "Microwave generation and power extraction in a magnetically insulated transmission line oscillator," *Bull. Amer. Phys. Soc.*, vol. 33, p. 1957, 1988.
[4] R. F. Harrington, *Time-Harmonic Electromagnetic Fields*. New York: McGraw-Hill, pp. 198–263, 1961.
[5] G. R. Gisler and M. E. Jones, "Charge-conserving algorithms versus Poisson corrections for electromagnetic PIC codes," presented at the 11th Int. Conf. on Numerical Simulation of Plasmas, Montreal, PQ, Canada, 1985.
[6] M. E. Jones and G. R. Gisler, "An implicit particle-in-cell algorithm for intense relativistic beam simulations," presented at the 11th Int. Conf. on Numerical Simulation of Plasmas, Montreal, PQ, Canada, 1985.
[7] G. R. Gisler, "Particle-in-cell simulations of azimuthal instabilities in relativistic electron layers," *Phys. Fluids*, vol. 30, pp. 2199–2208, 1987.
[8] D. Chernin and Y. Y. Lau, "Stability of laminar electron layers," *Phys. Fluids*, vol. 27, pp. 2319–2331, 1984.

*

Anthony L. Peratt (S'60–M'63–SM'85) was born in Belleville, KS, in 1940. He received the B.S.E.E. degree from California State Polytechnic University, Pomona, in 1963, the M.S.E.E. degree from the University of Southern California, Los Angeles, in 1967, and the Ph.D. degree in electrical engineering in 1971, also from the University of Southern California.

He was with the Aerospace Corp., Satellite Communications Group, and from 1972 to 1979 was a Staff Member at the Lawrence Livermore National Laboratory. He served as a Guest Scientist at the Max Planck Institute for Plasma Physics, Garching (1975–1977), and at the Department of Plasma Physics, The Royal Institute of Technology, Stockholm (1985). Since 1981 he has been with the Applied Theoretical Physics Division of the Los Alamos National Laboratory, Los Alamos, NM. His research interests have included wave coupling in nonuniform plasmas, diagnosis of plasmas with laser light and plasma holography, laser-plasma interaction theory, z pinches, and the particle-in-cell simulation of pulsed-power generators, magnetically insulated transmission lines, double layers, and microwave and synchrotron radiation from laboratory and astrophysical sources.

Dr. Peratt was Guest Editor of the IEEE TRANSACTIONS ON PLASMA SCIENCE Special Issue on Space and Cosmic Plasma (December 1986, April 1989), and Special Issue on Plasma Cosmology (February 1990); Guest Editor, *Laser and Particle Beams* Special Issue on Particle Beams and Basic Phenomena in the Plasma Universe (August 1988); and Session Organizer for Space Plasmas, IEEE International Conferences on Plasma Science, 1987–1989. He was elected to the IEEE Nuclear and Plasma Sciences Society ExCom, and holds membership in the American Physical Society, the American Astronomical Society, and Eta Kappa Nu.

*

Charles M. Snell was born in Elizabethton, TN, in 1946. He received the B.S. degree in physics from Vanderbilt University, Nashville, TN, in 1967, and the M.S. degree in astrophysics from the University of Arizona, Tuscon, in 1969.

He served with the Corps of Engineers Waterways Experiment Station from 1970 to 1974, and was a staff member at the Lawrence Livermore National Laboratory from 1974 to 1978. Since 1978 he has been with the Los Alamos National Laboratory, Los Alamos, NM. His research areas have included stellar photometry, solar system physics, dynamics of planetary cratering, and the use of computer codes to model and better understand complex physical phenomena. His current research interest is in the application of particle-in-cell simulation techniques to plasma physics and pulsed power systems.

*

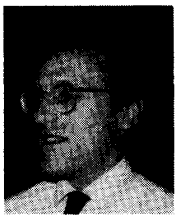

Franklin S. Felber received the A.B. (physics) degree from Princeton University, Princeton, NJ, in 1972, the M.A. (physics) degree from the University of Southern California, Los Angeles, in 1973, the M.S. (physics) degree from the University of Chicago in 1974, and the Ph.D. (physics) degree from the University of Southern California in 1975.

He has been Manager of the Directed Energy Division at JAYCOR, San Diego, CA, since 1984. He has published about two hundred papers and abstracts in pulsed power, accelerator and beam physics, plasma physics, fusion, nonlinear optics, laser-plasma interactions, and survivability.